

Phenomenological description of bidirectional surface reflection

Jan J. Koenderink and Andrea J. van Doorn

Helmholtz Institute, Utrecht University, P.O. Box 80 000, 3508 TA Utrecht, The Netherlands

Received January 26, 1998; revised manuscript received May 27, 1998; accepted June 29, 1998

General surface scattering is characterized through the bidirectional reflection distribution function (BRDF). The BRDF is a function of the directions of the incident and remitted beams and thus depends on four parameters. Under very general assumptions one shows that the BRDF is invariant under interchange of the incident and remitted beams, the so-called Helmholtz reciprocity. For isotropic surfaces the BRDF depends only on the absolute value of the difference between the azimuths of the incident and remitted beams. Since these exhaust the symmetries, the BRDF is a very complicated function. For many applications it would be advantageous to be able to summarize empirical data or to smooth and/or interpolate (often even extrapolate) BRDF data. We present a principled way to do this, exactly respecting the symmetry properties. © 1998 Optical Society of America [S0740-3232(98)01810-9]

OCIS codes: 240.6700, 290.0290, 120.5700, 120.5630.

1. INTRODUCTION

In applications such as remote sensing, computer vision, image interpretation, and computer graphics, one routinely deals with—in an optical sense—extremely complicated surfaces.¹⁻⁵ The very notion of surface depends on the scale of the problem: for instance, whether the surface might be of a leaf (near view), of a treetop (tree in a landscape view), or of a forest (in remote sensing from satellites). In some cases one has (usually approximate, phenomenological) models, but in most cases one simply depends on purely empirical data. One immediate problem is the sheer amount of data necessary to characterize arbitrary surface scattering. One conventionally represents general surface-scattering characteristics in terms of the bidirectional reflection distribution function (BRDF), which depends on the directions of both the incident and the remitted beams.⁶ One simply conceptualizes the collimated incident and remitted beams as subbeams of the actual source and detector configuration; the actual case then can be expressed as an integration over all such simple geometries with the BRDF as a weighting function. The BRDF is defined as the ratio of the radiance of the remitted beam to the irradiance of the surface caused by the incident beam. This definition makes solid physical sense because so-called Helmholtz reciprocity is expressed by the symmetry of the BRDF in the directions of the incident and remitted beams. Helmholtz reciprocity is a very general symmetry; it depends solely on the assumption of reversability of light rays and is thus of a purely geometrical nature.^{7,8} Empirically, all materials satisfy Helmholtz reciprocity within the experimental error. (However the general applicability of Helmholtz reciprocity has been doubted on both empirical and theoretical grounds; see Minnaert⁸ and Kortüm.³) For the general case this is the only symmetry of the BRDF. Quite often, statistical considerations suggest that the surface will be isotropic with respect to scattering. In such cases the BRDF depends only on the polar distances

of the incident and remitted beams (here we define the surface normal as the pole), whereas the azimuthal dependence is only on the absolute value of the difference between the azimuths of the incident and remitted beams. Although isotropy is by no means universal, it often applies in a statistical sense, at least to a reasonable approximation.¹

Because the BRDF has four degrees of freedom (e.g., the polar distances and azimuths of the incident and remitted beams), one requires a great amount of data to characterize it to some reasonable resolution. Suppose one desires an angular resolution ϵ (say); then approximately $(2\pi/\epsilon^2)^2/2$ data items are required (we divide by 2 because of Helmholtz reciprocity). For a resolution of 10° this already amounts to 2×10^4 numbers, for a resolution of 1° to 2×10^8 . This leads to a number of related problems: First, it takes great effort to collect such data. Consequently, full BRDF data are very scarce; in many cases the measurements have been confined to the plane of incidence. Second, even when the data are available it is inconvenient to use them. One needs principled methods for interpolation, extrapolation (when only plane-of-incidence data are available), smoothing, and summarizing. Often data are summarized through model fitting, but in many cases models are not (yet) available.

Whereas models of the physics are *in principle* always to be preferred (certainly when extrapolation is attempted), such models are not often available and when available only approximate, certainly for objects taken from the natural environment. What is worse, no single model can be expected to apply to all natural materials of interest. In this respect, phenomenological models are to be preferred *in practice*.

What is required is a principled method to summarize BRDF data in such a way that the symmetries (certainly Helmholtz reciprocity, often isotropy) are automatically respected when the description is coarse grained. This suggests a development in terms of orthonormal functions

on the direct product of the hemisphere (here denoted $\mathbf{H}_{\mathbf{S}^2}$) with itself (denoted $\mathbf{H}_{\mathbf{S}^2} \times \mathbf{H}_{\mathbf{S}^2}$). Such a basis should have a notion of order that naturally relates to angular resolution such that coarse graining (or smoothing) can be carried out through truncation or low-pass filtering. Whereas attempts have been made to use the spherical harmonics for this purpose, this remains at best a rather artificial device since the spherical harmonics are a complete orthogonal basis on the full unit sphere \mathbf{S}^2 instead of on the hemisphere $\mathbf{H}_{\mathbf{S}^2}$.

Since many bases for functions on $\mathbf{H}_{\mathbf{S}^2} \times \mathbf{H}_{\mathbf{S}^2}$ can be constructed, one may ask which one is the "best." To this question there cannot be given a general answer, since the set of possible functions (BRDF's) to represent is extremely large and it is not *a priori* clear what criterion is to be preferred. In practice, most natural materials have BRDF's that depend only slowly on the directions, suggesting that an orthonormal basis whose members have significant variations on only a limited range of scales is to be preferred. In that case omission of high-frequency components is likely to lead to efficient and good representations. Moreover, the representations will be slowly varying, which is indeed a requirement in cases where interpolation (or even moderate extrapolation) is attempted.

2. REPRESENTATION OF BIDIRECTIONAL REFLECTION DISTRIBUTION FUNCTIONS

A. Construction of an Orthogonal Basis for the Hemisphere

In optics, one often uses a complete, orthogonal basis on the unit disk \mathbf{D}^2 ; that is,

$$U_n^m(\rho, \phi) = \sqrt{\frac{2(n+1)}{\pi}} R_n^m(\rho) \cos m\phi, \quad m \geq 0, \tag{1}$$

$$U_n^m(\rho, \phi) = \sqrt{\frac{2(n+1)}{\pi}} R_n^m(\rho) \sin m\phi, \quad m < 0, \tag{2}$$

where the $R_n^{\pm m}(\rho)$ are the Zernike polynomials.⁹ Here the total order is n , whereas the upper index m denotes the azimuthal order. For the odd orders n , the index m may take any one of the values $m = -n, -n + 2, \dots, -1, +1, \dots, n - 2, n$, and for the even orders the values $m = -n, -n + 2, \dots, -2, 0, +2, \dots, n - 2, n$. Thus there are $n + 1$ distinct Zernike polynomials of the order n and thus $(n + 1)(n + 2)/2$ distinct polynomials up to (and including) order n . The polynomials are even or odd according to whether $|m|$ is even or odd. They contain only even or odd terms in ρ . The Zernike polynomials are closely related to the Jacobi polynomials, which are a terminating hypergeometric series. A closed expression for the Zernike polynomials is

$$R_n^{\pm m}(\rho) = \sum_{s=0}^{(n-m)/2} (-1)^s \frac{(n-s)!}{s! \left(\frac{n+m}{2} - s\right)! \left(\frac{n-m}{2} - s\right)!} \rho^{n-2s}. \tag{3}$$

In Eq. (1) we have adjusted the definition such that the basis is orthonormal; that is,

$$\int_{\mathbf{D}^2} U_n^k(\rho, \phi) U_m^l(\rho, \phi) dA = \delta_{nm} \delta_{kl}, \tag{4}$$

where dA is the area element of the unit disk. Notice that these functions naturally factor in a radial and an azimuthal part and that the azimuthal part reflects the properties of the rotation group faithfully: The azimuthal parts are simply the elements of the Fourier basis.

To avoid unduly long expressions, it is useful to introduce the azimuthal wave function $az_m(\phi)$ defined as

$$\begin{aligned} az_m(\phi) &= -\sin m\phi, & m < 0, \\ az_m(\phi) &= \frac{1}{\sqrt{2}}, & m = 0, \\ az_m(\phi) &= \cos m\phi, & m > 0. \end{aligned} \tag{5}$$

Of course, this can be avoided by using the complex dependence $\exp(im\phi)$ instead; however, we prefer to work with real-valued functions throughout. Notice that we have

$$\int_{-\pi}^{+\pi} az_n(\phi) az_m(\phi) d\phi = \pi \delta_{nm}. \tag{6}$$

We will also have frequent occasion to use the relation

$$az_n(\phi + \pi) = \begin{cases} az_n(\phi), & n \text{ even} \\ -az_n(\phi), & n \text{ odd} \end{cases} \tag{7}$$

It is easily possible to use this basis for the unit disk \mathbf{D}^2 to construct a basis for the hemisphere $\mathbf{H}_{\mathbf{S}^2}$; after all, the disk and the hemisphere are topologically equivalent and geometrically very similar. Notice that the area element of the disk in the conventional polar coordinates is $dA = \rho d\rho d\phi$, whereas the element of solid angle on the hemisphere in the conventional spherical polar coordinates is $d\Omega = \sin \theta d\theta d\phi$. Because of the identity

$$2 \sin \frac{\theta}{2} d\left(2 \sin \frac{\theta}{2}\right) = \sin \theta d\theta, \tag{8}$$

from elementary differential calculus we can easily establish a relation. Notice that we have

$$\int_0^{\pi/2} R_n^k \left(\sqrt{2} \sin \frac{\theta}{2}\right) R_m^k \left(\sqrt{2} \sin \frac{\theta}{2}\right) \sin \theta d\theta = \frac{\delta_{nm}}{n+1}. \tag{9}$$

Let $U(\rho, \phi) = R(\rho)\Phi(\phi)$ be a function on the unit disk and $W(\theta, \phi) = \Theta(\theta)\Psi(\phi)$ a function on the hemisphere. Then

$$\Theta(\theta) = \frac{1}{2} R \left(\sqrt{2} \sin \frac{\theta}{2}\right), \tag{10}$$

$$\Psi(\phi) = \Phi(\phi) \tag{11}$$

defines a relation such that

$$\int_{\mathbf{D}^2} U(\rho, \phi) dA = \int_{\mathbf{H}_{\mathbf{S}^2}} W(\theta, \phi) d\Omega. \tag{12}$$

What happens here is that we essentially use the area-true mapping of the sphere on the plane that is due to Lambert. When we apply this to the basis for the unit disk \mathbf{D}^2 , we obtain a complete, orthonormal basis for the hemisphere $\mathbf{H}_{\mathbf{S}^2}$. The basis functions are (see Figs. 1 and 2)

$$K_n^l(\theta, \phi) = \sqrt{\frac{n+1}{\pi}} R_n^l \left(\sqrt{2} \sin \frac{\theta}{2} \right) a_{zl}(\phi). \quad (13)$$

By construction we have

$$\int_{\mathbf{H}_{\mathbf{S}^2}} K_n^k(\theta, \phi) K_m^l(\theta, \phi) d\Omega = \delta_{nm} \delta_{kl}. \quad (14)$$

Thus the basis is orthonormal. The basis is also complete because its preimage on the unit disk is complete.

Because we have constructed a complete, orthonormal basis on the hemisphere with desirable symmetry properties (the azimuthal dependence respects the structure of the group of rotations about the polar axis), we are now able to represent arbitrary scalar functions of directions at one side of a planar interface. This system should have many applications in radiometry (and transport

theory in general). In this paper we will use it to construct practical representations for BRDF's.

B. General Surface-Scattering Modes

As noted earlier the BRDF is defined as the radiance of the remitted beam divided by the irradiance caused by the incident beam⁶:

$$f(\theta_i, \phi_i, \theta_r, \phi_r) = \frac{dN_r(\theta_r, \phi_r)}{dH_i(\theta_i, \phi_i)}, \quad (15)$$

the subscripts denoting the incident (*i*) and the remission (*r*) directions. Because of its definition the BRDF may become singular, especially in the case of grazing incidence. A common example is the case of perfect specular reflection. In such cases it is often preferable to work with the function

$$g(\theta_i, \phi_i, \theta_r, \phi_r) = f(\theta_i, \phi_i, \theta_r, \phi_r) \cos \theta_i, \quad (16)$$

which is the remitted radiance that is due to irradiance by a collimated source of constant intensity. In such cases we may seek a development of the function *g* instead of the function *f* in terms of a complete orthonormal basis.

In developing the BRDF, we may simply set

$$f(\theta_i, \phi_i, \theta_r, \phi_r) = \sum_{mkl} a_{nm}^{kl} \frac{K_n^k(\theta_i, \phi_i) K_m^l(\theta_r, \phi_r) + K_n^k(\theta_r, \phi_r) K_m^l(\theta_i, \phi_i)}{(2 + 2\delta_{nm} \delta_{kl})^{1/2}}. \quad (17)$$

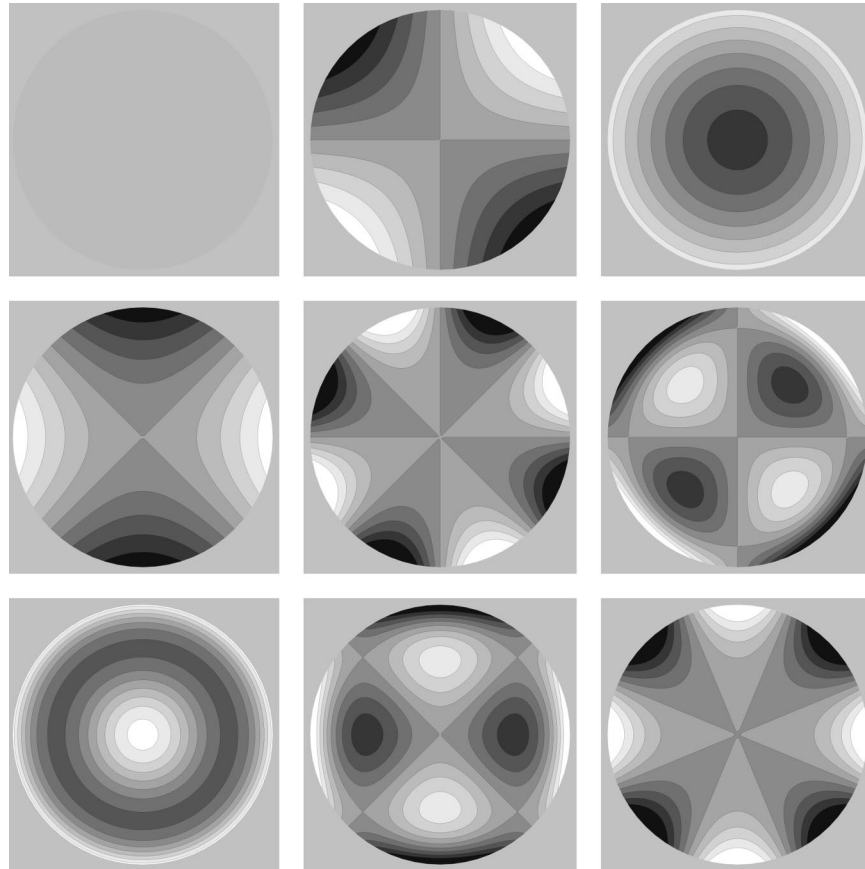


Fig. 1. Contour density plots of the orthonormal basis functions $K_n^l(\theta, \phi)$ for even orders *n* up to 4. From left to right and top to bottom, the plots show K_0^0 , K_2^{-2} , and K_2^0 (top row); K_2^2 , K_4^{-4} , and K_4^0 (center row); K_4^4 , K_4^2 , and K_4^4 (bottom row). The odd orders are shown in Fig. 2.

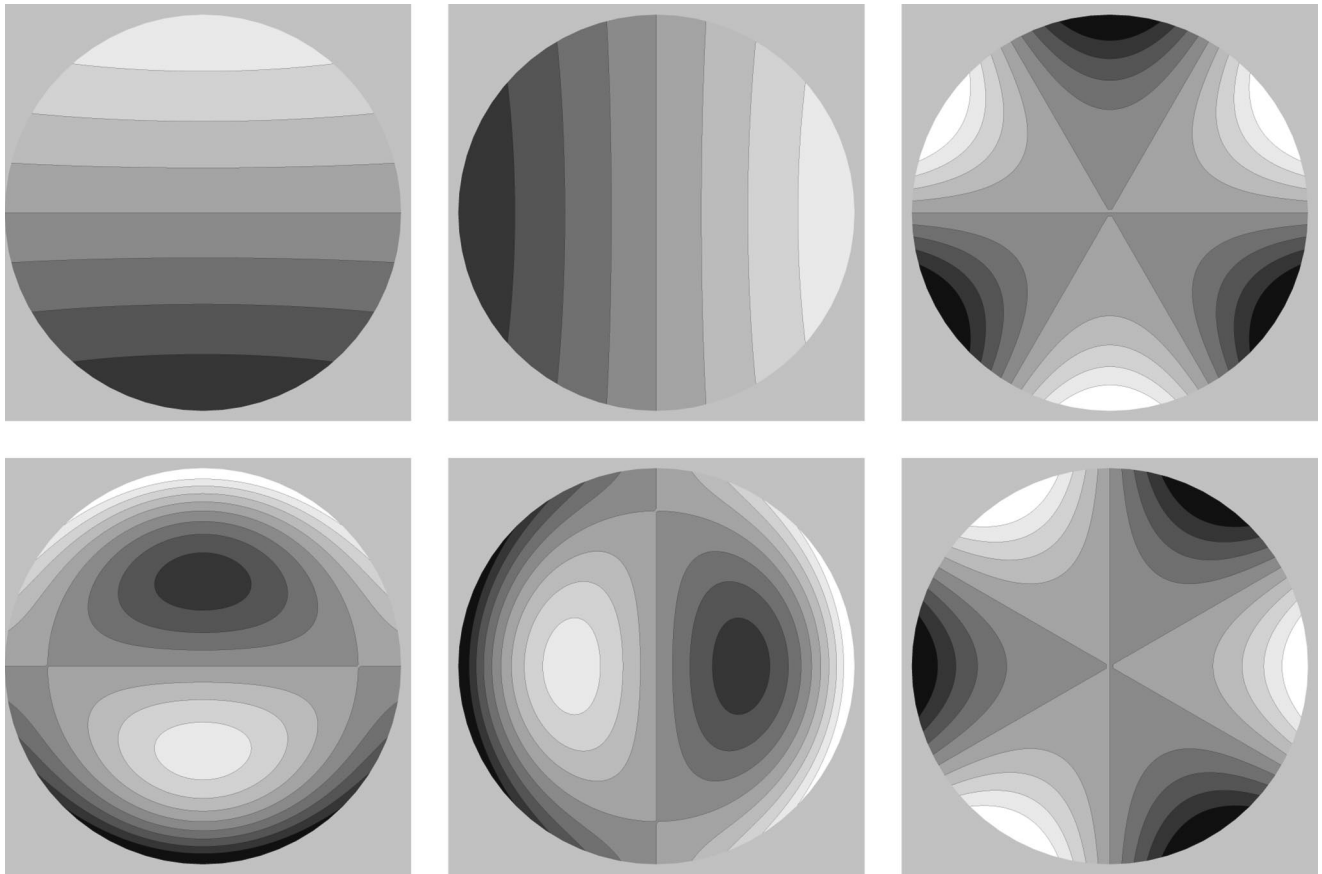


Fig. 2. Contour density plots of the orthonormal basis functions $K_n^l(\theta, \phi)$ for odd orders n up to 4. From left to right and top to bottom, the plots show K_1^{-1} , K_1^1 , and K_3^{-3} (top row); K_3^{-1} , K_3^1 , and K_3^3 (bottom row). The even orders are shown in Fig. 1.

We will refer to the functions

$$H_{nm}^{kl}(\theta_i, \phi_i, \theta_r, \phi_r) = \frac{K_n^k(\theta_i, \phi_i)K_m^l(\theta_r, \phi_r) + K_n^k(\theta_r, \phi_r)K_m^l(\theta_i, \phi_i)}{(2 + 2\delta_{nm}\delta_{kl})^{1/2}}, \tag{18}$$

as Helmholtz surface-scattering modes. In terms of the Zernike polynomials and azimuthal wave functions, we have

$$H_{nm}^{kl}(\theta_i, \phi_i, \theta_r, \phi_r) = \frac{1}{\pi} \left[\frac{(n+1)(m+1)}{2 + 2\delta_{nm}\delta_{kl}} \right]^{1/2} \times \left[R_n^k \left(\sqrt{2} \sin \frac{\theta_i}{2} \right) R_m^l \left(\sqrt{2} \sin \frac{\theta_r}{2} \right) az_k(\phi_i) az_l(\phi_r) + R_m^l \left(\sqrt{2} \sin \frac{\theta_i}{2} \right) R_n^k \left(\sqrt{2} \sin \frac{\theta_r}{2} \right) az_l(\phi_i) az_k(\phi_r) \right]. \tag{19}$$

By construction one has

$$\int_{\mathbf{H}_s^2 \times \mathbf{H}_s^2} H_{nm}^{kl}(\theta_i, \phi_i, \theta_r, \phi_r) \times H_{n'm'}^{k'l'}(\theta_i, \phi_i, \theta_r, \phi_r) d\Omega_i d\Omega_r = \delta_{nn'} \delta_{mm'} \delta_{kk'} \delta_{ll'}. \tag{20}$$

Although the functions $K_n^k(\theta_i, \phi_i)K_m^l(\theta_r, \phi_r)$ represent a complete orthogonal basis for the direct product of the

hemisphere with itself, the Helmholtz surface-scattering modes are a basis of the subspace of functions to which Helmholtz reciprocity pertains. (One can easily show that the direct sum of the mutually orthogonal linear subspaces of symmetric and antisymmetric combinations spans the space.) In developing any empirically determined BRDF (which might violate Helmholtz reciprocity due to scatter in the data) we automatically project on this subspace and thus discard components that violate Helmholtz reciprocity as noise. The development yields the closest function that fits the data yet respects reciprocity in the least-squares sense. We obtain the coefficients in the development through projection on the Helmholtz surface-scattering modes:

$$a_{nm}^{kl} = \int_{\mathbf{H}_s^2 \times \mathbf{H}_s^2} f(\theta_i, \phi_i, \theta_r, \phi_r) \times H_{nm}^{kl}(\theta_i, \phi_i, \theta_r, \phi_r) d\Omega_i d\Omega_r. \tag{21}$$

The list of coefficients $\{a_{nm}^{kl}\}$ represents the bidirectional surface-scattering spectrum, or (upholding the tradition set by the BRDF) the BSSS. The BSSS characterizes the bidirectional surface reflection in a way that is reminiscent of the Fourier spectrum in the sense that increasing order stands for increasing resolution. Thus the low-order spectrum yields the overall properties, whereas the high-order spectrum specifies detail. For empirically determined BRDF's the BSSS will be very noisy at the high orders, and in most cases a truncation (smoothing)

will improve the description. Here we meet with the most obvious advantage of the spectral representation: It is trivial (indeed automatic) to obtain summary descriptions that respect the data and Helmholtz reciprocity at the same time. Such summary descriptions represent the best estimates in the least-squares sense.

The BSSS can be naturally factored into polar and azimuthal parts. The order nm refers to the polar part. For each order nm there are $(n + 1)(m + 1)$ azimuthal spectral components. We define the total order N as $N = \max\{n, m\}$. There are $(N + 1)^2(N + 2)^2/4$ spectral components of total order N . Thus the number of spectral components that we have to reckon with rises very steeply (asymptotically with the fourth power) with the total order indeed. A rough estimate of the resolution obtained with the BSSS truncated at total order N is $\epsilon \approx 4/(N + 1)$. For total order 8 we find $\epsilon \approx 25^\circ$. This is close to the practical limit in most applications.

C. Surface-Scattering Modes for Isotropic Scattering

When the surface may be regarded as isotropic, the number of independent spectral components is drastically reduced. In the case of isotropic scattering, the azimuthal dependence is only on the absolute difference $\Delta\phi_{ir} =$

$|\phi_i - \phi_r|$ of the azimuths of the incident and remitted beam directions. Thus the azimuthal dependence is as $\cos m\Delta\phi_{ir}$. Of course, Helmholtz reciprocity also applies (it applies in any case), and thus we have to select a basis for the subspace of Helmholtz surface-scattering modes with the desired azimuthal symmetry. The required complete and orthonormal basis is (see Table 1)

$$I_{nm}^l(\theta_i, \theta_r, \Delta\phi_{ir}) = \frac{1}{2\pi} \left[\frac{(n + 1)(m + 1)}{A_{nm}^l} \right]^{1/2} \times \left[R_n^l \left(\sqrt{2} \sin \frac{\theta_i}{2} \right) R_m^l \left(\sqrt{2} \sin \frac{\theta_r}{2} \right) + R_m^l \left(\sqrt{2} \sin \frac{\theta_i}{2} \right) R_n^l \left(\sqrt{2} \sin \frac{\theta_r}{2} \right) \right] \times \cos l\Delta\phi_{ir}. \tag{22}$$

$$A_{nm}^l = \begin{cases} 4 & \text{if } (n = 0) \text{ or } ((n = m) \text{ and } (l = 0)) \\ 2 & \text{if } ((n = m) \text{ or } (l = 0)) \\ 1 & \text{otherwise} \end{cases}. \tag{23}$$

Table 1. Isotropic Surface-Scattering Modes up to Order 4

$$I_{00}^0(\theta_i, \theta_r, \Delta\phi_{ir})^a = \frac{1}{2\pi}$$

$$I_{11}^1(\theta_i, \theta_r, \Delta\phi_{ir}) = \frac{2\sqrt{2}}{\pi} \sin \frac{\theta_i}{2} \sin \frac{\theta_r}{2} \cos \Delta\phi_{ir}$$

$$I_{20}^0(\theta_i, \theta_r, \Delta\phi_{ir}) = \frac{1}{\pi} \sqrt{\frac{3}{2}} \left(2 \sin^2 \frac{\theta_i}{2} + 2 \sin^2 \frac{\theta_r}{2} - 1 \right)$$

$$I_{22}^0(\theta_i, \theta_r, \Delta\phi_{ir}) = \frac{3}{2\pi} \left(4 \sin^2 \frac{\theta_i}{2} - 1 \right) \left(4 \sin^2 \frac{\theta_r}{2} - 1 \right)$$

$$I_{22}^2(\theta_i, \theta_r, \Delta\phi_{ir}) = \frac{6\sqrt{2}}{\pi} \sin^2 \frac{\theta_i}{2} \sin^2 \frac{\theta_r}{2} \cos 2\Delta\phi_{ir}$$

$$I_{31}^1(\theta_i, \theta_r, \Delta\phi_{ir}) = \frac{4\sqrt{2}}{\pi} \sin \frac{\theta_i}{2} \sin \frac{\theta_r}{2} \left(3 \sin^2 \frac{\theta_i}{2} + 3 \sin^2 \frac{\theta_r}{2} - 2 \right) \cos \Delta\phi_{ir}$$

$$I_{33}^1(\theta_i, \theta_r, \Delta\phi_{ir}) = \frac{16\sqrt{2}}{\pi} \sin \frac{\theta_i}{2} \sin \frac{\theta_r}{2} \left(3 \sin^2 \frac{\theta_i}{2} - 1 \right) \left(3 \sin^2 \frac{\theta_r}{2} - 1 \right) \cos \Delta\phi_{ir}$$

$$I_{33}^3(\theta_i, \theta_r, \Delta\phi_{ir}) = \frac{16\sqrt{2}}{\pi} \sin^3 \frac{\theta_i}{2} \sin^3 \frac{\theta_r}{2} \cos 3\Delta\phi_{ir}$$

$$I_{40}^0(\theta_i, \theta_r, \Delta\phi_{ir}) = \frac{1}{\pi} \sqrt{\frac{5}{2}} \left(12 \sin^4 \frac{\theta_i}{2} + 12 \sin^4 \frac{\theta_r}{2} - 6 \sin^2 \frac{\theta_i}{2} - 6 \sin^2 \frac{\theta_r}{2} + 1 \right)$$

$$I_{42}^0(\theta_i, \theta_r, \Delta\phi_{ir}) = \frac{1}{\pi} \sqrt{\frac{15}{2}} \left(2 \sin^2 \frac{\theta_i}{2} + 2 \sin^2 \frac{\theta_r}{2} - 1 \right) \left(24 \sin^2 \frac{\theta_i}{2} \sin^2 \frac{\theta_r}{2} - 6 \sin^2 \frac{\theta_i}{2} - 6 \sin^2 \frac{\theta_r}{2} + 1 \right)$$

$$I_{42}^2(\theta_i, \theta_r, \Delta\phi_{ir}) = \frac{4\sqrt{15}}{\pi} \sin^2 \frac{\theta_i}{2} \sin^2 \frac{\theta_r}{2} \left(4 \sin^2 \frac{\theta_i}{2} + 4 \sin^2 \frac{\theta_r}{2} - 3 \right) \cos 2\Delta\phi_{ir}$$

$$I_{44}^0(\theta_i, \theta_r, \Delta\phi_{ir}) = \frac{5}{2\pi} \left(24 \sin^4 \frac{\theta_i}{2} - 12 \sin^2 \frac{\theta_i}{2} + 1 \right) \left(24 \sin^4 \frac{\theta_r}{2} - 12 \sin^2 \frac{\theta_r}{2} + 1 \right)$$

$$I_{44}^2(\theta_i, \theta_r, \Delta\phi_{ir}) = \frac{10\sqrt{2}}{\pi} \sin^2 \frac{\theta_i}{2} \sin^2 \frac{\theta_r}{2} \left(8 \sin^2 \frac{\theta_i}{2} - 3 \right) \left(8 \sin^2 \frac{\theta_r}{2} - 3 \right) \cos 2\Delta\phi_{ir}$$

$$I_{44}^4(\theta_i, \theta_r, \Delta\phi_{ir}) = \frac{40\sqrt{2}}{\pi} \sin^4 \frac{\theta_i}{2} \sin^4 \frac{\theta_r}{2} \cos 4\Delta\phi_{ir}$$

^aFor numerical work these functions would be written in Horner's normal form in terms of the parameters $\sin^2 \theta_i$ and $\sin^2 \theta_r$.

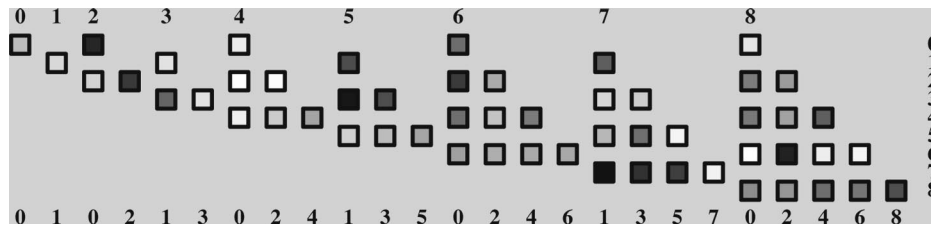


Fig. 3. Example of an IBSSS, illustrating a layout that permits a quick overview of the spectral composition of an isotropic BRDF. The order n runs from left to right (the numbers on the top row), and the associated order m runs from top to bottom (the numbers in the column on the right). The azimuthal order l also runs from left to right but starts anew for every new order n . The magnitude of the spectral components is given by the gray level; medium gray (background) defines the zero level.

Table 2. Values of n , m , l for Isotropic Surface-Scattering Modes up to Order 4

Spectral Component	Order				
n	0	1	222	333	444444
m	0	1	022	133	022444
l	0	1	002	113	002024

We may develop BRDF's as

$$f(\theta_i, \theta_r, \Delta\phi_{ir}) = \sum_{nm} a_{nm}^l I_{nm}^l(\theta_i, \theta_r, \Delta\phi_{ir}), \quad (24)$$

with

$$a_{nm}^l = \int_{\mathbf{H}_s^2 \times \mathbf{H}_s^2} f(\theta_i, \theta_r, \Delta\phi_{ir}) \times I_{nm}^l(\theta_i, \theta_r, \Delta\phi_{ir}) d\Omega_i d\Omega_r. \quad (25)$$

We obtain the isotropic bidirectional surface-scattering spectrum (IBSSS); see Fig. 3.

The restrictions on the indices are

$$n \geq 0, \quad 0 \leq m \leq n, \quad 0 \leq l \leq m \\ (n-l), (m-l) \text{ even}; \quad (26)$$

thus there are not nearly as many spectral components in the IBSSS as there are in the BSSS. There exist only 5 spectral components of total order 2 (instead of 14), 14 of total order 4 (instead of 55) and 55 of total order 8 (instead of 295). The spectral components up to total order 4 are listed in Table 2. It will thus be much easier to interpret the IBSSS than it will be to interpret the BSSS. In most cases it will be advantageous to split the BSSS into an isotropic part (essentially the IBSSS) and an anisotropic part. One expects the contribution of the anisotropic part to be typically much smaller than that of the isotropic part.

3. APPLICATIONS

A. Modal Descriptions

In order to describe BRDF data intuitively, one often uses a modal description, where the modes or lobes have some immediate physical relevance.¹⁰⁻¹⁶ Easily the best-known instance is the description of smooth interfaces between air and some opaque dielectric bulk material in terms of a specular lobe and a Lambertian scattering. Here the specular lobe is thought to arise from Fresnel re-

flection at the interface, whereas the Lambertian component is thought to be due to radiation that has suffered multiple scatterings in the volume of the material. For rough interfaces, where vignetting becomes relevant, one often adds a backscatter lobe, which is thought to be due to the fact that no cast shadow should be visible from the direction of the incident beam. Such modal descriptions are intuitive and are closely related to idealized surface models. It is clearly important to establish a connection between the BSSS and such modal descriptions.

1. Lambertian Lobe

The BRDF for a Lambertian surface¹⁷ of unit albedo is a constant that is equal to $1/\pi$. In this case we can write down the BSSS by inspection because the Lambertian BRDF is in the direction of the zeroth-order surface-scattering mode and orthogonal to all others. The only nonvanishing spectral component at order zero equals $\frac{1}{2}\sqrt{2}$.

Thus the dc term of the BSSS is simply the Lambertian lobe itself. Reversing this, the Lambertian BRDF is simply the lowest-order approximation of any BRDF. Of course this fits in very well with conventional practice.

2. Specular Lobe

For a perfect mirror the BRDF becomes singular, and we prefer to use the function $g(\theta_i, \phi_i, \theta_r, \phi_r)$ defined above. We have¹²

$$g(\theta_i, \phi_i, \theta_r, \phi_r) = \frac{\delta(\theta_r - \theta_i)\delta(\phi_i - \phi_r + \pi)}{\sin \theta_r}. \quad (27)$$

The delta functions specify the reflection law, whereas the factor is needed to take care of the fact that the radiances of the incident and reflected beams are equal.

Because of the delta functions in the integrand, it is an easy matter to do the integrals in order to find the spectral components:

$$\int_{\mathbf{H}_s^2 \times \mathbf{H}_s^2} g(\mathbf{r}_i, \mathbf{r}_r) H_{nm}^{kl}(\mathbf{r}_i, \mathbf{r}_r) d\Omega_i d\Omega_r. \quad (28)$$

Integrating over the delta functions yields

$$\frac{1}{\pi} \left[\frac{(n+1)(m+1)}{(2+2\delta_{nm}\delta_{kl})} \right]^{1/2} \\ \times \int_0^{\pi/2} \sin \theta R_n^k \left(\sqrt{2} \sin \frac{\theta}{2} \right) R_m^l \left(\sqrt{2} \sin \frac{\theta}{2} \right) d\theta$$

$$\begin{aligned} & \times \int_0^{2\pi} (az_k(\phi)az_l(\phi - \pi) + az_l(\phi)az_k(\phi - \pi))d\phi \\ & = \frac{(-1)^k}{\pi} \delta_{nm} \delta_{kl}. \end{aligned} \quad (29)$$

Thus we find that—as expected—the spectrum is isotropic. All (isotropic) spectral components except those of the form $\{n, n, k\}$ vanish, and the absolute values of the nonvanishing spectral components are all equal to each other. Thus the specular lobe has a flat IBSSS diagonal spectrum, much like the Fourier spectrum of an impulse. The simplicity of the result of course derives from the assumption of an ideal specular surface: In the case in which the reflection coefficient depends on the direction (as in Fresnel reflection), the expressions become more complicated (though the integration is still quite feasible).

We add that the even components of the form $\{n, n, 0\}$ can be written in terms of Legendre polynomials since we have the identity

$$R_{2n}^0(\rho) = P_n(2\rho^2 - 1). \quad (30)$$

This makes the purely diagonal spectra especially simple to analyze.

In Fig. 4 we plot the approximations to the ideal-mirror BRDF obtained through truncation of the development after order 0, 1, 2, 4, 6, 8, or 16. For the lowest order we have simply the Lambertian (totally diffusing) surface: The reflected radiation is isotropically distributed, and no specularity is apparent. As the higher orders are added, we first see an asymmetry developing (more radiation is returned in the general direction of the reflected beam) and then an obvious mode, centered on the ideally reflected ray. As higher and higher orders are added, it is mainly the angular width of this lobe that changes: It

becomes narrower and narrower as the order increases. Owing to the abrupt truncation, there is some evidence of the expected ringing effect. It is evident that dropping the high-order terms in the series leads to a rather graceful degradation of the ideal-mirror BRDF.

In Fig. 5 we plot the approximation truncated after order 8 for various angles of incidence. As is evident from these figures, this approximation indeed follows the law of specular reflection quite well. The ringing caused by the abrupt truncation of the series is seen to depend on the precise geometry. Notice that severe ringing may produce negative spurious lobes. This is indeed to be expected from *any* linear method. Such problems do not arise in the case of realistic BRDF's of practical interest. In extreme cases such as truly specular surfaces, physical models are of course the more logical choice. The width of the lobe depends on the order at which the series is truncated: Of course an infinite number of terms would be required to capture true specularity. As in Fourier synthesis, there is a simple relation between width and order.

3. Backscatter Lobe

Consider an ideal backscatter: The remitted beam is in the direction of the incident beam and has the same radiance. Approximate examples are retroreflective surfaces coated with glass beads or corner cubes as are sometimes used for traffic signs in some countries. The BRDF is similar to that of a perfect mirror, except for the fact that we have to change the reflection law into a retroreflection law:

$$g(\theta_i, \phi_i, \theta_r, \phi_r) = \frac{\delta(\theta_r - \theta_i)\delta(\phi_i - \phi_r)}{\sin \theta_r}. \quad (31)$$

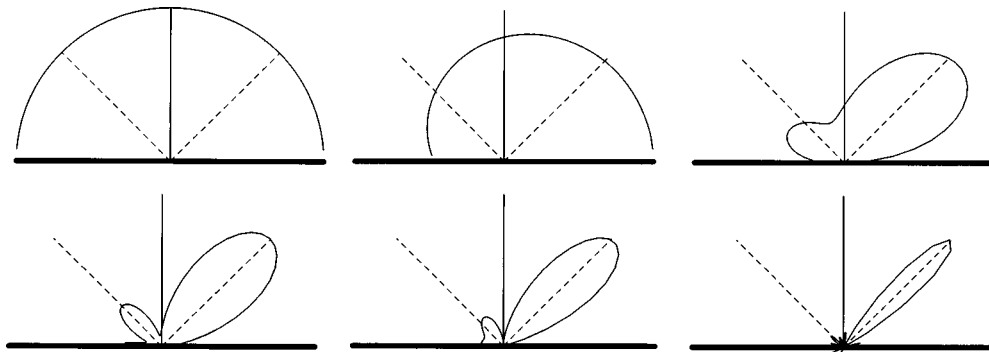


Fig. 4. Truncated series of the ideal mirror with the addition of a small Lambertian component. Orders 0, 1, and 2 are depicted on the top row, orders 4, 6, and 8 on the bottom row. The angle of incidence is 45° for all plots. Notice the pronounced specular lobe for orders 2 and higher, growing narrower with increasing order. Also notice the ringing due to abrupt truncation of the series (the small spurious lobes in directions other than that of the reflected ray). Such ringing can be damped through a more gradual attenuation of the amplitudes, just as with the familiar Fourier series.

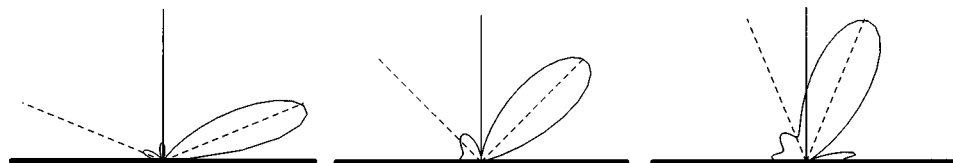


Fig. 5. Truncated series of the ideal mirror with the addition of a small Lambertian component for only terms of order 8 and lower. The angle of incidence is 67.5° (left), 45° (middle), and 22.5° (right). Notice that the approximation neatly satisfies the reflection laws and that the precise structure of the ringing depends on the geometry (angle of incidence).

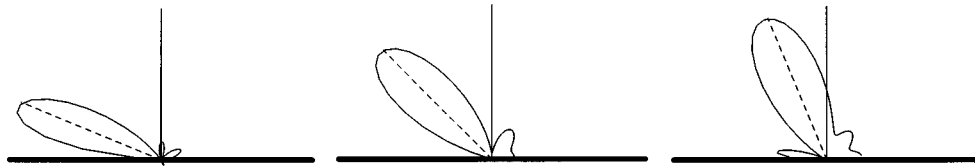


Fig. 6. Truncated series of the ideal retroreflector with the addition of a small Lambertian component for only terms of order 8 and lower. The angle of incidence is 67.5° (left), 45° (middle), and 22.5° (right). Notice that the approximation neatly satisfies the ideal backscatter laws and that the precise structure of the ringing depends on the geometry (angle of incidence).

Again, owing to the presence of the delta functions in the integrand, we can immediately carry out all the necessary integrations:

$$\int_{\mathbf{H}_{\mathbb{S}^2} \times \mathbf{H}_{\mathbb{S}^2}} g(\mathbf{r}_i, \mathbf{r}_r) H_{nm}^{kl}(\mathbf{r}_i, \mathbf{r}_r) d\Omega_i d\Omega_r \quad (32)$$

$$= \frac{1}{\pi} \left[\frac{(n+1)(m+1)}{(2+2\delta_{nm}\delta_{kl})} \right]^{1/2} \int_0^{\pi/2} \sin \theta R_n^k \left(\sqrt{2} \sin \frac{\theta}{2} \right)$$

$$\times R_m^l \left(\sqrt{2} \sin \frac{\theta}{2} \right) d\theta \quad (33)$$

$$\times 2 \int_0^{2\pi} az_k(\phi) az_l(\phi) d\phi = \frac{1}{\pi} \delta_{nm} \delta_{kl}. \quad (34)$$

We find that—as expected—the spectrum is isotropic. All (isotropic) spectral components except those of the form $\{n, n, k\}$ vanish, and these nonvanishing spectral components are all equal to each other. Thus the backscatter lobe has a flat IBSSS diagonal power spectrum.

The properties of the backscatter development are very similar indeed to those of the ideal mirror (as was to be expected given the similarities of the structure of these BRDF's). In Fig. 6 we plot the approximation obtained by truncation of the series after order 8 for various angles of incidence. As is evident from these plots, the approximation has a well-developed backscatter lobe centered about the direction of ideal backscattering.

B. Smoothing of Bidirectional Reflection Distribution Function Data

BRDF data can be smoothed by truncation of the BSSS. A problem that might occur is ringing, when the spectrum actually extends beyond the truncation order. In such cases a low-pass BSSS filter is to be preferred. Examples of ringing can be easily illustrated with the BSSS of the perfect mirror. Because the specular BSSS is flat, truncation at any order will result in more or less serious ringing effects. This is clearly visible in Figs. 4–6.

We have used truncation of the BSSS to smooth a large body of empirical BRDF's (approximately 50 natural materials). A full description of the data is available.¹ These data have been made publicly available on the internet at www.cs.columbia.edu/cave/curet. Each BRDF is represented as a list of 205 data items, and each data item holds the BRDF values in three broad spectral bands. Full photometric and geometric calibration is provided.

All BRDF's in the CURET database were fitted to order 2 (5 free parameters) and order 8 (55 free parameters). The results of the fit are also included in the database. Many BRDF's are well represented by the order 2 fit, and

all BRDF's are accurately fitted by the order 8 fit. The conclusion is that it will rarely be necessary to consider total order in excess of 8 in the BSSS; in most cases order 2 or 4 will amply suffice. The data have also been fitted with a model of the physics⁵ that assumes a Lambertian surface on the microscale but surface modulations (V-shaped grooves in all directions) on the macroscale. The model accounts for self-occlusion, shadowing, and interreflections. Many of the natural materials can be fitted quite well by this simple model, but others clearly violate the assumptions and are not represented very well. When the model applies, the BRDF's are represented with fewer free parameters than are required for the phenomenological description. However, the phenomenological description captures all cases without fail.

C. Extrapolation from Plane-of-Incidence Data

In many cases of practical interest, only BRDF data for plane-of-incidence geometries are available. In such cases, one would like to (or one might *have to*) extrapolate the data to include cases where the incident and remitted beam fail to be co-planar with the surface normal. In such cases, one may project the BSSS data on the basis and thus obtain an estimate of the BSSS; however, many spectral components will turn out to be identically zero because no data projects on them. We may assign these spectral components random values and still end up with a valid BSSS in the sense that the data do not allow any inference concerning these components. Clearly the choice of least commitment is to be preferred; thus we assign zero value to these spectral components. The BSSS then allows us to extrapolate from the data in a unique manner. Notice that such an extrapolation depends on faith rather than on physics: When available at all, a model of the physics is always to be preferred. However, a least-committed phenomenological extrapolation is often the only way out. It is indeed widely used in practice when arbitrary surfaces are treated as Lambertian, with an albedo obtained from only a few measurements or only one measurement. This corresponds to truncation after the first term in the present representation. Thus our method can be seen as a refinement of a method that is already widely used in practice without any formal backing.

We used this type of extrapolation in a recent study on the BRDF of velvet. Only plane-of-incidence data were available. These could be very accurately fitted with total order 8. A large number of spectral components were indeed trivially identically zero (because the data were limited to the plane of incidence), but many others were found empirically to be negligible. A very good fit was provided with only about a dozen spectral components.

This description lets us extrapolate BRDF values to arbitrary (out of the plane of incidence) geometries.

D. Summary Description of Physical Models

Physical models of realistic surfaces will often result in very complicated BRDF's, usually with nonanalytic components. This is almost a necessity because such models (except in very simple cases such as scattering from shallow Gaussian random surfaces) have to incorporate the geometry of vignetting (cast shadow and visual occlusion), which results in nonanalyticity.^{13,14,18} Typically solutions are patched together from a number of cases among which one decides on the basis of source and viewing geometry. The sheer complexity of such models usually makes their actual formal representation irrelevant; one uses only their numerical predictions. In such cases it might well be preferable to compute the BSSS of the model (numerically of course) and replace the model with a standard approximation in terms of surface-scattering modes.

Of the many expressions that have been proposed to account for the scattering of radiation by natural surfaces, a great many can be exactly represented in terms of BSSS's. The simplest example is of course Lambert's law (a constant); another well-known instance is Öpik's formula (or rather Minnaert's generalization of it)^{8,19}:

$$f(\theta_i, \phi_i, \theta_r, \phi_r) = \frac{k+1}{2\pi} (\cos \theta_i \cos \theta_r)^{k-1} \quad (0 \leq k \leq 1). \quad (35)$$

Clearly the BSSS terminates, and thus the representation in terms of surface-scattering modes will be exact. This is also the case for many reflection models in common use in computer graphics today.^{20,21}

For other well-known models such as those of Beckmann and Spizzichino¹⁰ and Torrance and Sparrow,¹⁶ the BSSS does not terminate and an infinite series is required. In such cases good approximations can be obtained by truncation or low-pass filtering.

4. DISCUSSION

We have presented a novel method to represent bidirectional surface-scattering data that has a number of advantages. It is a rational method that automatically guarantees that the symmetries of the physics are respected (Helmholtz reciprocity and perhaps isotropy) and that yields a spectral description graded with respect to angular resolution such that smoothing results from truncation or low-pass filtering. Immediate application areas include the representation, smoothing, and extrapolation of empirical data. (Summary) data representation might indeed be a primary application area. We believe that the resulting spectrum (BSSS) is of considerable importance in its own right and can be used advantageously to characterize BRDF data when surface analysis is the issue. Current methods are based on an informal decomposition into modes (Lambertian component, specular lobe, backscatter lobe, and so forth). Using the BSSS allows much more precise language. Moreover, the conventional modes can easily be identified in the BSSS.

For instance, the dc term is simply the Lambertian lobe, the reflection lobe appears as a flat spectral distribution, and so forth. Thus the spectral interpretation need not be less intuitive than the modal analysis and is clearly to be preferred.

When the hemisphere of directions is tessellated into equal-area faces [one possibility is through barycentric subdivision of the (triangular) faces of the regular (hemi-)icosahedron], the integrals turn into summations and the description in terms of surface-scattering modes can be formalized as simple linear algebra in which BRDF's occur as matrices that can be implemented as lookup tables. The theory developed in this paper can be immediately converted into such discrete formalizations that might be highly desirable in computer graphics applications.

We have put this theory into practice in the analysis of a large body of BRDF data on a variety of natural and synthetic materials (building materials, foodstuffs, plant canopies, cloth, paper, etc.). Data and results of the analysis (including BRDF fits with the surface-scattering modes discussed in this paper) are available as a public database (www.cs.columbia.edu/cave/curet). Excellent fits are obtained in all cases; typically order 4 (or less) suffices, but in some cases order 8 is required for the data to be fitted within the empirical tolerances.

REFERENCES

1. K. J. Dana, B. van Ginneken, S. K. Nayar, and J. J. Koenderink, "Reflectance and texture of real-world surfaces," Columbia U. Tech. Rep. CUCS-048-96 (Columbia University, New York, 1996).
2. L. da Vinci, *Treatise on Painting*, A. P. McMahon, transl. (Princeton U. Press, Princeton, N.J., 1959).
3. G. Kortüm, *Reflectance Spectroscopy*, J. E. Lohr, transl. (Springer-Verlag, Berlin, 1969).
4. S. K. Nayar, K. Ikeuchi, and T. Kanade, "Surface reflection: physical and geometrical perspectives," *IEEE Trans. Pattern Anal. Mach. Intell.* **13**, 611–634 (1991).
5. S. K. Nayar and M. Oren, "Visual appearance of matte surfaces," *Science* **267**, 1153–1156 (1995).
6. F. E. Nicodemus, J. C. Richmond, J. J. Hsia, I. W. Ginsberg, and T. Limperis, "Geometrical considerations and nomenclature for reflectance," NBS Monograph 160 (National Bureau of Standards, Washington, D.C., 1977).
7. H. L. F. von Helmholtz, *Treatise on Physiological Optics* (Dover, New York, 1962), Vol. I, p. 231.
8. M. Minnaert, "The reciprocity principle in lunar photometry," *Astrophys. J.* **93**, 403–410 (1941).
9. M. Born and E. Wolf, *Principles of Optics* (Pergamon, London, 1959).
10. P. Beckmann and A. Spizzichino, *The Scattering of Electromagnetic Waves from Rough Surfaces* (Pergamon, New York, 1963).
11. B. K. P. Horn and M. J. Brooks, *Shape from Shading* (MIT Press, Cambridge, Mass., 1989).
12. B. K. P. Horn and R. W. Sjoberg, "Calculating the reflectance map," *Appl. Opt.* **18**, 1770–1779 (1979).
13. M. Oren and S. K. Nayar, "Generalization of the Lambertian model and implications for machine vision," *Int. J. Comput. Vis.* **14**, 227–251 (1995).
14. M. Oren and S. K. Nayar, "Generalization of Lambert's reflectance model," *ACM Comput. Graphics (SIGGRAPH 94)*, 239–246 (1994).
15. H. D. Tagare and R. J. P. deFigueiredo, "A theory of photometric stereo for a class of diffuse non-Lambertian surfaces," *IEEE Trans. Pattern Anal. Mach. Intell.* **13**, 133–152 (1991).

16. K. E. Torrance and E. M. Sparrow, "Theory of off-specular reflection from roughened surfaces," *J. Opt. Soc. Am.* **57**, 1105–1114 (1967).
17. J. H. Lambert, *Photometria sive de mensura de gradibus luminis, colorum et umbræ* (Eberhard Klett, Augsburg, Germany, 1760).
18. B. G. Smith, "Geometrical shadowing of a random rough surface," *IEEE Trans. Antennas Propag.* **AP-15**, 668–671 (1967).
19. E. Öpik, "Photometric measures of the moon and the earth-shine" [Publications de L'Observatoire Astronomical de L'Université de Tartu (Estonia), 1924], Vol. 26, pp. 1–68.
20. J. F. Blinn, "Models of light reflection for computer synthesized pictures," *ACM Comput. Graphics (SIGGRAPH 77)*, 542–547 (1977).
21. R. L. Cook and K. E. Torrance, "A reflectance model for computer graphics," *ACM Comput. Graphics* **15**, 309–328 (1982).